ISSN 1062-8738, Bulletin of the Russian Academy of Sciences: Physics, 2025, Vol. 89, No. 9, pp. 1632–1638. © Pleiades Publishing, Ltd., 2025.

Gas Combustion in Two-Layer Cylindrical Burner with Return by Radiative Heat Exchange

S. S. Minaev[a, b], E. P. Dats[c, *], and S. N. Mokrin[b, d]

[a] *Lebedev Physical Institute, Russian Academy of Sciences, Moscow, 119991 Russia*

[b] *Far Eastern Federal University, Vladivostok, 690091 Russia*

[c] *Vladivostok State University, Vladivostok, 690014 Russia*

[d] *Institute of Applied Mathematics, Far Eastern Branch, Russian Academy of Sciences, Vladivostok, 690041 Russia*

**e-mail: datsep@gmail.com*

Received November 30, 2024; revised December 13, 2024; accepted May 23, 2025

Abstract—We theoretically estimated the maximum achievable efficiency of radiative burners with filtration gas combustion in a porous medium. The theoretical estimates obtained for a cylindrical burner with two coaxial porous shells, between which the flame is stabilized, and for a single-layer porous burner with filtration combustion of combustion gas. In the first case, heat regeneration is carried out due to radiation heat exchange between the layers, and in the second case, it occurs due to the thermal conductivity of the porous frame. It has been shown that the radiation efficiency of the burners is approximately the same and does not depend on the heat recovery way. At the same time, a two-layer system has an obvious advantage over a single-layer burner due to significantly lower material consumption and lower hydraulic losses when filtering gas through a porous medium.

Keywords: gas combustion, porous media, radiative heat exchange, heat return, burner efficiency

DOI: 10.1134/S1062873825712346

INTRODUCTION

The gas combustion in systems with heat return from combustion products to the combustible mixture without mixing them is widely used in practical burners. Various schemes of burners with heat return are described in [1–4] and others.

Researchers' interest in such systems is due to the possibility of lean gas mixtures burning, achieving superadiabatic temperatures and creating burners with low emissions of harmful substances (NO_x, CO) into the atmosphere. One of well know method for burners' production is self-propagating high-temperature synthesis (SHS) which is the alternative of spark plasma sintering for manufacturing of intermetallic and ceramic materials [5, 6]. Processes with heat return also include filtration gas combustion. The theory and experimental study of combustion processes in such systems were developed in [7–10]. Heat recirculation during filtration gas combustion occurs due to the heat transfer from combustion products through a porous medium to the preheating zone, where the combustible mixture is heated by heat exchange with the porous medium. Then the heated combustible mixture enters the chemical reaction zone, and after combustion, part of the combustion products heat is returned to the porous medium. This method of heat return is widely described in the literature and it explains the possibility of lean gas mixtures burning [11] and achievement of superadiabatic temperatures in the gas combustion zone [12]. To stabilize the flame inside a porous burner, a cylindrical [13–15] configuration of burners with a radial supply of the combustible mixture to the center of the burner is often used. This configuration makes it possible to create a diverging radial gas flow and stabilize the filtration gas combustion wave inside the porous frame. Porous burners make it possible to effectively convert combustion heat into thermal radiation, which, unlike the heat carried away by the convective flow of combustion products, is convenient to use in energy-converting devices, for processing materials and other applications [16, 17]. Therefore, an important task is to assess the efficiency of a radiation burner, which is the ratio of the thermal radiation flux to the heat flux released during combustion of the fuel mixture.

Typical cylindrical burners are hollow, cigar-shaped, porous shells within which gas combustion occurs [13]. The thickness of such shells rarely exceeds several centimeters and the gas combustion often occurs not inside the outer porous shell, but in the internal space between the combustible mixture supply system and the porous shell.

In this case, the heat recovery mechanism as during filtration gas combustion is no longer possible, since

the combustion of the mixture occurs in front of the porous medium that exclude the heat return from combustion products to the fresh mixture via heat exchange with porous shell. At the same time, the preheating of the combustible mixture can be due to radiative heat transfer from the outer shell to the combustible mixture supply system inside the burner, which transfers heat to the incoming combustible gas. It is due to such heat regeneration in thin-walled porous burners that it is possible to achieve superadiabatic temperatures and burn extremely lean mixtures. This method of heat recovery and its effect on combustion characteristics are poorly described in the literature.

This work is devoted to assessing of the radiant burners efficiency with the return of combustion products heat to the combustible mixture through radiation heat exchange between the outer shell and the combustible mixture supply system. In experiments or in practical burners, injection is carried out through a nozzle connected to a heat-conducting platform. In the idealized model, we will assume that the gas combustion occurs in the space between two coaxial cylindrical porous shells. The combustible mixture is fed through the inner shell, which is heated by radiation from the outer porous shell. Gas combustion occurs between two coaxial cylindrical porous layers, and the hot combustion products exit radially through the outer porous layer into the environment. Radiation from the outer porous layer goes both outside, into the surrounding space, and inside the burner, where it heats the inner porous shell. The combustible mixture is heated by the internal porous layer and enters the combustion zone at an elevated temperature. This heat return mechanism allows lean mixtures to be burned and combustion to be stabilized.

This work compares the characteristics of a cylindrical porous burner with filtration gas combustion and a two-layer porous burner with radiation heat return.

MATHEMATICAL MODEL

The problem is solved within the framework of a two-temperature thermal-diffusion model [7, 8]. Stationary heat equations for gas and solid phase and diffusion equation for deficient reactant have the form:

$$\rho_g c_{pg}\frac{r_0 V_0}{mr}\frac{\partial T_g}{\partial r} = \lambda_g\left(\frac{1}{r}\frac{\partial T_g}{\partial r}+\frac{\partial^2 T_g}{\partial r^2}\right) + \rho_g Q W(Y,T_g) - \frac{\alpha}{d_p}(T_g - T_s), \quad (1)$$

$$\lambda_s\left(\frac{1}{r}\frac{\partial T_s}{\partial r}+\frac{\partial^2 T_s}{\partial r^2}\right)+\frac{\alpha}{d_s}(T_g - T_s) = 0, \quad (2)$$

$$\frac{r_0 V_0}{mr}\frac{\partial Y}{\partial r} = D_c\left(\frac{1}{r}\frac{\partial Y}{\partial r}+\frac{\partial^2 Y}{\partial r^2}\right) - W(Y,T_g). \quad (3)$$

The equations are written in the cylindrical coordinates under the assumption that all quantities depend only on the radial coordinate r. The indices s and g refer to the porous media and the gas, respectively. The inlet gas velocity into porous medium is v_0 and the gas mass velocity $(\rho_g v r)$ is a constant value. It is considered that the heat capacities c_{ps}, c_{pg}, thermal conductivity coefficients λ_g, λ_s and the density of the solid porous medium ρ_s do not depend on temperature. The heat transfer coefficient between gas and porous medium is determined by the relation $\alpha = (\lambda_g Nu)/d_p$ where Nu is Nusselt number, d_p is the average pore size, d_s is the characteristic size of an element of a porous medium. The porosity m is determined by the relationship. $D_c = \lambda_g/(c_{pg}\rho_g)$ is fuel diffusion coefficient in lean combustible mixture. The rate of one-step chemical reaction is set as $W(Y,T_g) = AY\exp\left(-\frac{E_a}{T_g R}\right)$, where Y is the concentration of deficient reactant in combustible mixture; N_a is activation energy; R is universal gas constant and A is pre-exponential factor. Q is thermal effect of chemical reaction.

Equations (1)–(3) are supplemented with boundary conditions at the boundaries of the porous medium. The problem is solved for two geometric configurations. In the case (a), the filtration gas combustion occurs inside a cylindrical porous layer and in the case (b), the gas combustion occurs in the free space between two cylindrical layers. The gas combustion diagram is shown in Figs. 1a and 1b.

For both configurations, it is assumed that there is an internal volume $r_0 < r < r_1$, into which a premixed fuel-air mixture is supplied. In the case of one-layer porous media (it is shown in Fig. 1a) when the combustion occurs inside porous media $r_1 < r < r_4$, the boundary conditions read:

$$r = r_0: Y = Y_0,\ \ T_g = T_0;\ \ r = r_1: \frac{\partial T_s}{\partial r} = 0; \quad (4)$$

$$r = r_4: -\lambda_s\frac{\partial T_s}{\partial r} = \varepsilon\sigma\left(T_s^4 - T_0^4\right), \quad \frac{\partial T_g}{\partial r} = 0,\ \ \frac{\partial Y}{\partial r} = 0. \quad (5)$$

Here ε is the emissivity of the outer shell, and σ_{SB} is the Stefan–Boltzmann constant. On the internal and external surfaces of the porous medium $r = r_1$ and $r = r_4$ the gas temperature T_g and concentration Y are continuous.

In the case when combustion occurs in a volume between two porous shells, as shown in Fig. 1b, conditions (4), (5) are supplemented by conditions at the boundaries $r = r_2$ and $r = r_3$. Taking into account the radiative heat exchange between the surfaces $r = r_2$

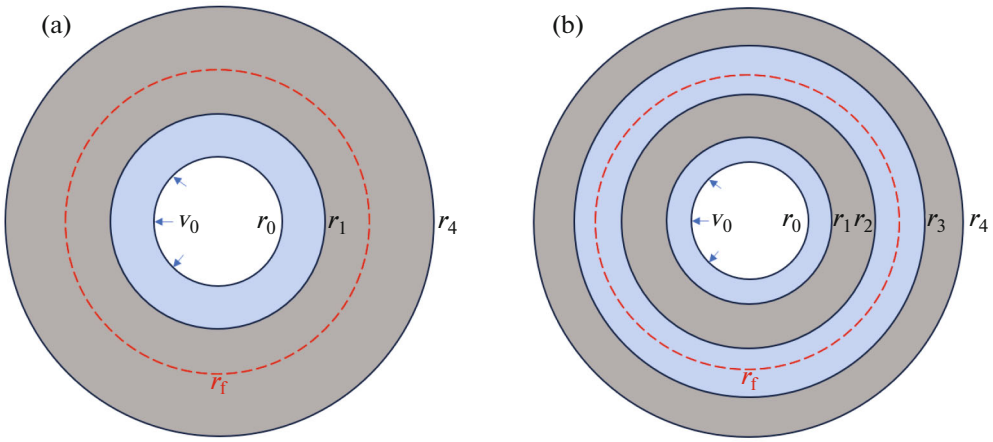

Fig. 1. Scheme of the computational domain: (a) one-layer burner; (b) two-layer burner. Areas with a porous medium are marked in gray, and free space is marked in blue.

and $r = r_3$, the conditions for heat fluxes at the boundaries of porous shells have the form:

$$r = r_2: \lambda_s \frac{\partial T_s(r_2)}{\partial r} = -\frac{q}{r_2}\left(T_s^4(r_2) - T_s^4(r_3)\right), \quad (6)$$

$$r = r_3: \lambda_s \frac{\partial T_s(r_3)}{\partial r} = -\frac{q}{r_3}\left(T_s^4(r_2) - T_s^4(r_3)\right). \quad (7)$$

In the areas where there is no porous medium $r_0 < r < r_1$, $r_2 < r < r_3$, the porosity m is equal to one $m = 1$. During combustion under adiabatic conditions, the temperature of the mixture is equal to the adiabatic temperature T_b, therefore the energy flow entering the burner with the combustible mixture is equal to $v_0 r_0 \rho_g c_{pg}(T_b - T_0)$, the thermal radiation flux from a unit of the external surface of the burner is equal to $\varepsilon(1-m) r_4 \sigma_{SB}\left(T_s^4(r_4) - T_0^4\right)$. The efficiency of the radiation burner is calculated by the equation:

$$\eta = \frac{\varepsilon(1-m) r_4 \sigma_{SB}\left(T_s^4(r_4) - T_0^4\right)}{v_0 r_0 \rho_g c_{pg}(T_b - T_0)} \times 100\%. \quad (8)$$

To calculate the efficiency by Eq. (8) it is necessary to calculate the wall temperature $T_s(r_4)$. The temperature value $T_s(r_4)$ can be estimated as follows. Let's multiply Eq. (3) by $\rho_g Q$, Eq. (2) by d_s/d_p and add these equations with Eq. (1). The resulting equation will be:

$$\frac{\rho_g v_0 r_0}{mr}\frac{d}{dr}(c_{pg} T_g + QY) = \left(\frac{1}{r}\frac{d}{dr} + \frac{d^2}{dr^2}\right)\left(\lambda_g T_g + \rho_g Q D_c Y + \lambda_s \frac{d_s}{d_p} T_s\right). \quad (9)$$

Let us now multiply (9) by r and integrate the resulting equation from $r = r_0$ to $= r_4$, taking into account conditions (4)–(7) at the boundaries of porous layers. As a result of integration, one can obtain the law of conservation of energy in the form:

$$\frac{\rho_g v_0 r_0}{m} c_{pg}\left(T_g(r_4) - T_b\right) = -r_4 \frac{d_s}{d_p} \varepsilon \sigma_{SB}\left(T_s^4(r_4) - T_0^4\right). \quad (10)$$

Taking into account (10), the expression for burner efficiency (8) can be written in the form

$$\eta = \frac{T_b - T_g(r_4)}{T_b - T_0} \times 100\%. \quad (11)$$

Note that the maximum possible burner efficiency can be estimated from the following considerations. As follows from the calculations given in the next section, the temperature of the combustion products decreases with distance from the flame, and the temperature of the porous medium in the outer shell monotonically increases, but always remains less than the gas temperature. In the limiting case of a very large shell thickness and the absence of radiation heat loss to the environment, the temperature of the porous medium and gas will be equal to the adiabatic temperature. Since, according to Eq. (8), the burner efficiency monotonically increases with increasing surface temperature $T_s(r_4)$, then for an upper estimate of the efficiency by Eq. (8) one can assume that the gas temperature is equal to the porous layer temperature at its outer boundary $T_g(r_4) = T_s(r_4) = T^*$ [19].

An estimate of the maximum burner temperature T^* can be found from solving the equation that follows from the law of conservation of energy (10) under the condition $T_g(r_4) = T_s(r_4) = T^*$:

$$r_4 \frac{d_s}{d_p} \varepsilon \sigma_{SB}\left((T^*)^4 - T_0^4\right) + \frac{\rho_g v_0 r_0}{m} c_{pg}(T^* - T_b) = 0. \quad (12)$$

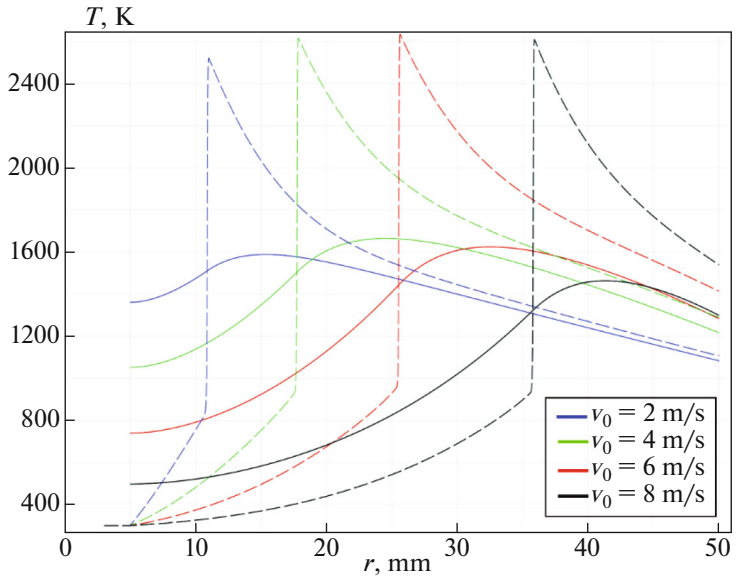

Fig. 2. Temperature distributions of the gas (dashed curve) and the porous frame (solid curve), calculated for different gas inlet velocities v_0. The radii of the porous burner are $r_1 = 5$ mm and $r_4 = 50$ mm.

Then substituting the value of T^* into Eq. (11) or (8) one can obtain an estimate of the maximum efficiency.

NUMERICAL SIMULATION

The calculation was carried out using the finite element analysis program Comsol Multiphysics. The search for solution of Eqs. (1)–(3) is implemented using the establishment method. In this method the time derivative is added to the left sides of the equations and, using a variable time step, a stationary solution is sought. Initial time step is $dt = 10^{-6}$ s. The computational domain consists of finite elements of the same size, having a length $dl = 2\times10^{-5}$ m.

The initial conditions in the calculations had the form:

$$r_1 < r < 0.5(r_1 + r_4):$$
$$T_g(r,t_0) = T_s(r,t_0) = T_0, Y(r,t_0) = Y_0;$$
$$0.5(r_1 + r_4) < r < r_4:$$
$$T_g(r,t_0) = T_s(r,t_0) = T_b, Y(r,t_0) = 0.$$

Calculations were performed for the following values of the problem parameters: $r_0 = 3$ mm, $m = 0.5$, $Nu = 4$, $dp = 1$ mm, $c_{pg} = 1200$ J/(kg K), $\lambda_g = 0.03$ W/(m K) and $\lambda_s = 10$ W/(m K). Initial gas temperature $T_0 = 300$ K, adiabatic flame temperature is $T_b = 2000$ K, heat of reaction $Q = 46\times10^6$ J/kg, pre-exponential factor $A = 10^8$ s^{-1} and the activation energy $N_a = 12.5\times10^5$ J/mol in reaction rate approximately corresponded to a methane-air mixture with a equivalence ratio $\varphi = 0.8$.

RESULTS AND DISCUSSION

Let us consider a single-layer porous burner with gas combustion inside a porous medium $r_1 < r < r_4$ (Fig. 1a). Figure 2 shows the temperature distributions of the gas and the porous frame at different inlet gas velocities v_0. The dashed line indicates the temperature of the gas mixture and the solid line indicates the temperature of the porous frame.

Figure 2 demonstrates that the gas combustion occurs at a superadiabatic temperature (adiabatic temperature is $T_b = 2000$ K), the maximum value of which is almost irrespective to the gas flow. An increase in gas flow rate shifts the combustion zone closer to the outer surface of the burner and leads to increase of the gas and the porous shell temperatures.

Let's consider the temperature distribution in a two-layer burner (Fig. 1b) in which the combustion of the mixture occurs between two porous shells. To compare the characteristics of two burners, calculations were performed at the same values of the gas input velocity v_0 and the same radii r_1 and r_4. The radii of the first layer are $r_1 = 5$ mm and $r_2 = 10$ mm, and the radii of the second layer are $r_3 = 40$ mm and $r_4 = 50$ mm. Figure 3 shows the distributions of the gas temperature (dashed line) and the temperature of the porous shells (solid line).

Just as in the case of filtration gas combustion in a single-layer porous burner, gas combustion in the free

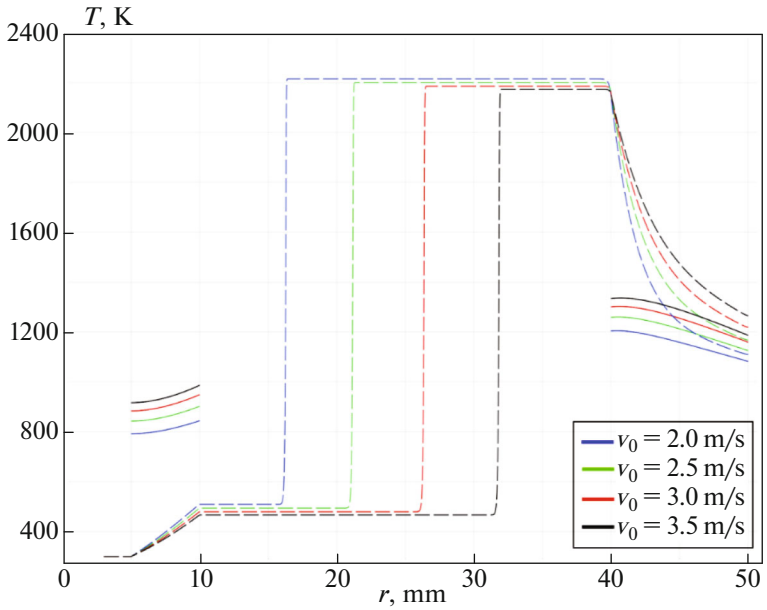

Fig. 3. Temperature distributions of the gas (dashed curve) and the porous layers (solid curve), calculated for different velocities v_0 of the inlet flow of the combustible mixture.

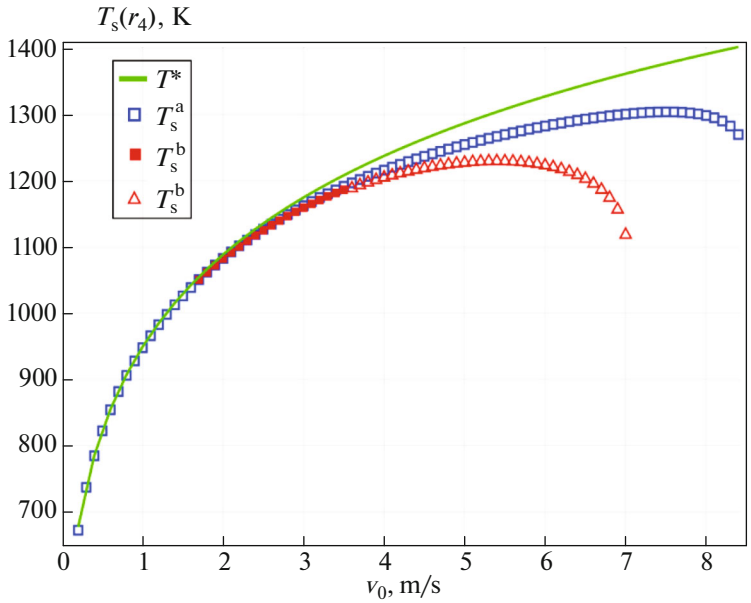

Fig. 4. The temperature of one-layer T_s^a and the temperature T_s^b of two-layer burners depending on the input gas velocity v_0. The solid green line is temperature T^*, calculated by Eq. (12).

space between two re-emitting porous layers occurs at the superadiabatic temperature. The maximum gas temperature in a two-layer system increases as the gas supply rate to the burner decreases, while in a single-layer porous burner, the maximum gas temperature increases with increasing flow rate of the combustible mixture. Note that the maximum gas temperature of the filtration combustion wave in a single-layer system (Fig. 2) significantly exceeds the maximum gas combustion temperature between porous layers (Fig. 3). The temperature difference for the selected set of parameters is 15%.

Figure 4 shows solid surface temperature at the outlet of single-layer and double-layer burners depending on the input flow velocity of the combustible mixture, and the temperature T^* calculated using the approximate Eq. (12). Red solid squares show the surface temperature of the double-layer burner in the case of gas combustion between the layers, and red tri-

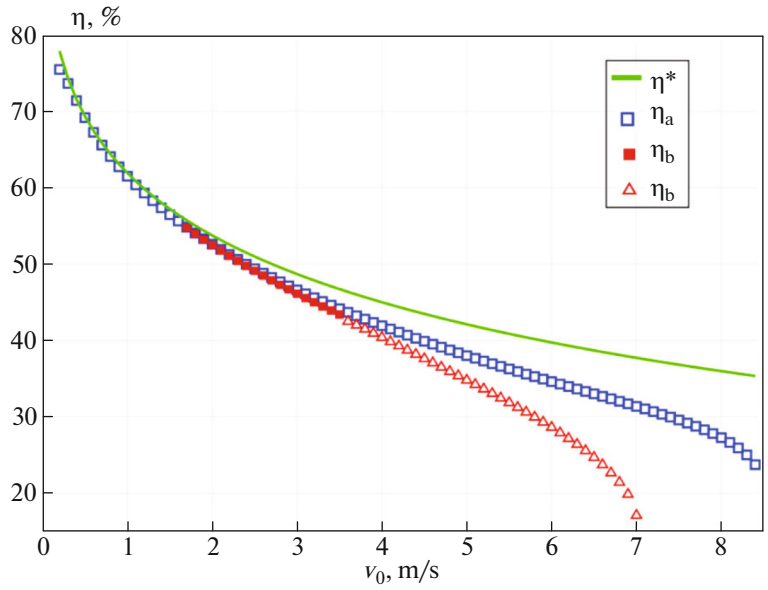

Fig. 5. The radiation efficiency of one-layer η_a and the efficiency η_b of two-layer burners depending on the input gas velocity v_0. The solid green line is the efficiency η^*, calculated by Eq. (12).

angles show the surface temperature during filtration gas combustion inside the second shell.

Figure 5 shows the radiation efficiency of the single-layer and double-layer burners depending on the input flow velocity of the combustible mixture, as well as the radiation efficiency, calculated by Eq. (12). The calculations show that the radiation efficiency decreases with increasing the flow rate of combustible mixture. The filtration gas combustion in a one-layer burner exists when the input gas velocity varies in the range from 0.2 to 8.4 m/s. In two-layer burner the gas combustion occurs between two porous layer when the input gas velocity varies from 1.7 to 3.5 m/s and the filtration gas combustion in the outer porous layer exists for the range of input gas velocity from 3.6 to 7 m/s. The minimum possible flow rate in a two-layer system is determined by the case when the velocity of the combustible gas at the exit from the inner cylindrical shell is approximately equal to the normal velocity of the laminar flame. If the velocity of the combustible mixture flowing from the outer shell becomes less than the normal flame velocity, then the flame will not be able to stabilize between the shells. Case when the flame is stabilized in the inner porous shell are not considered, since the inner shell is often used as a flame preventer. The maximum velocity in a two-layer burner is selected from the condition under which the flame can exist in the gap between the two shells and does not enter the filtration gas combustion mode in the outer shell. Note that the characteristics of a two-layer burner are close to the characteristics of a single-layer burner when the gas combustion occurs in the space between two porous layers. In this case the maximum difference in efficiencies of two type burners is less than 1%. The minimum efficiency, as follows from the calculations shown in Fig. 4, corresponds to the maximum possible gas velocity, which is achieved when the flame is established near the inner surface of the outer shell. Note that the difference between the maximum efficiency η^* calculated by Eq. (12) and the efficiencies found in numerical simulations increases as gas flow increases. This fact is explained by more efficient heat exchange between the gas and the porous medium at low flow rates leading to reduction of the temperatures difference of the exhaust gases and the porous layer outer surface. At the same time the aproximate Eq. (12) allows us to estimate the efficiency and temperature of outer surface of porous burners with good accuracy in the case when burners efficiency is near to maximal one.

These results show that heat recovery through radiative heat exchange between shells of two layers burner achieve performance similar to that of single-layer burners. At the same time, double shell burners obviously have less weight compared to thick single-layer porous burners, which have similar performance characteristics. In addition, the gas ignition in the space between the shells in a two-layer burner is a fairly simple procedure compared to initiating filtration gas combustion inside a porous layer in a single-layer burner, which requires prolonged heating of the porous medium. Two-layer porous burner has reduced hydraulic resistance compared to a single-layer burner that, in some cases, makes it possible to avoid the use of a compressor to increase the pressure of the combustible mixture before feeding it into the burner and to use simpler injection methods for supplying the combustible mixture.

CONCLUSIONS

Theoretical estimates of radiation efficiency for cylindrical porous burners in two typical configurations were obtained. In the first case, filtration gas combustion occurs inside a porous shell, which transfers heat from the combustion products to the combustible mixture due to the heat-conducting porous media. This heat recovery mechanism is well known from numerous works on filtration gas combustion. In the second burner configuration, gas combustion occurs in the free space between two porous shells with thermal coupling due to radiation heat exchange. The mechanism of heat return from combustion products to the fresh mixture is carried out due to radiation heat exchange between the shells. The obtained results demonstrate that this method of heat recovery allows to achieve performance similar to that used in single-porous- layer burners. The work obtained efficiency estimates and other characteristics for burners with two re-emitting shells. Estimates for two types of burners were made based on calculations within the framework of a two-temperature model of filtration gas combustion in a porous medium. Qualitative dependences of the burner efficiency on the main problem parameters were obtained for a cylindrical burner with two coaxial porous shells and a single-layer porous burner with filtration gas combustion. It has been shown that the radiation efficiency of the burners is approximately the same and does not depend on the method of heat recovery. At the same time, a two-layer system has an advantage over a single-layer burner due to significantly lower hydraulic losses when filtering gas through it. Reduced hydraulic losses, fast flame initiation in the space between the shells, reduction in material consumption and weight of two-layer burners compared to a single-layer burner make the use of such burners promising in practical applications.

FUNDING

This study was supported by the Ministry of Science and Higher Education of the Russian Federation (project no. FZNS-2024-0003).

CONFLICT OF INTEREST

The authors of this work declare that they have no conflicts of interest.

REFERENCES

1. Lloyd, S. and Weinberg, F., *Nature*, 1974, vol. 251, p. 47. https://doi.org/10.1038/251047a0
2. Jones, A., Lloyd, S., and Weinberg, F., *Proc. R. Soc.*, 1978, vol. 360, p. 97.
3. Takeno, T. and Haae, K., *Combust. Sci. Technol.*, 1983, vol. 31, p. 207. https://doi.org/10.1080/00102208308923642
4. Lloyd, S., *Ind. Eng. Chem. Res.*, 1994, vol. 33, p. 1809. https://doi.org/10.1021/ie00031a021
5. Gurin, M.S., Shtarev, D.S., Shtareva, A.V., et al., *Bull. Russ. Acad. Sci.: Phys.*, 2023, vol. 87, p. 390. https://doi.org/10.1134/S1062873823705925
6. Shevtsova, L.I., Esikov, M.A., Gavrilov, A.I., et al., *Bull. Russ. Acad. Sci.: Phys.*, 2024, vol. 88, p. 1465. https://doi.org/10.1134/S1062873824707700
7. Babkin, V., Drobushevich, V., Laevskii, Y., and Potytnyakov, S., *Combust. Explos. Shock Waves*, 1983, vol. 19, p. 147. https://doi.org/10.1007/BF00789228
8. Howell, J., Hall, M., and Ellzey, J., *Prog. Energy Combust. Sci.*, 1996, vol. 22, p. 121. https://doi.org/10.1016/0360-1285(96)00001-9
9. Trimis, D. and Durst, F., *Combust. Sci. Technol.*, 1996, vol. 121, p. 153. https://doi.org/10.1080/00102209608935592
10. Kamal, M. and Mohamad, A., *J. Power Energy*, 2006, vol. 220, p. 487. https://doi.org/10.1243/09576509JPE169
11. Wood, S. and Harris, A., *Prog. Energy Combust. Sci.*, 2008, vol. 34, p. 667. https://doi.org/10.1016/j.pecs.2008.04.003
12. Kennedy, L., Fridman, A., and Saveliev, A., *Int. J. Fluid Mech. Res.*, 1995, vol. 22, p. 1. https://doi.org/10.1615/InterJFluidMechRes.v22.i2.10
13. Fursenko, R., Maznoy, A., Odintsov, E., Kirdyashkin, A., Minaev, S., and Kumar, S., *Intern. J. Heat Mass Transfer*, 2016, vol. 98, p. 277. https://doi.org/10.1016/j.ijheatmasstransfer.2016.03.048
14. Palesskii, F., Fursenko, R., and Minaev, S., *Combust. Explos. Shock Waves*, 2014, vol. 50, p. 625. https://doi.org/10.1134/S001050821406001X
15. Dobrego, K., Zhdanok, S., and Futko, S., *Int. J. Heat Mass Transfer*, 2000, vol. 43, p. 3469.
16. Banerjee, A. and Paul, D., *Energy*, 2021, vol. 221, p. 119868. https://doi.org/10.1016/j.energy.2021.119868
17. Gharehghani, A., Ghasemi, K., Siavashi, M., and Mehranfar, S., *Fuel*, 2021, vol. 304, p. 121411. https://doi.org/10.1016/j.fuel.2021.121411
18. Dats, E. and Minaev, S., *Int. J. Heat Mass Transfer*, 2022, vol. 195, p. 123141. https://doi.org/10.1016/j.ijheatmasstransfer.2022.12314
19. Maznoy, A., Kirdyashkin, A., Minaev, S., Markov, A., Pichugin, N., and Yakovlev, E., *Energy*, 2018, vol. 160, p. 399. https://doi.org/10.1016/j.energy.2018.07.017

Publisher's Note. Pleiades Publishing remains neutral with regard to jurisdictional claims in published maps and institutional affiliations.
AI tools may have been used in the translation or editing of this article.